

## RESEARCH ARTICLE

# Catalytic reduction of 4-nitrophenol using synthesized and characterized CoS@MorphcdtH/CoS@4-MPipzcdtH nanoparticles

Gunjan Chauhan<sup>1</sup> | Suvarcha Chauhan<sup>2</sup> | Surbhi Soni<sup>1</sup> | Anand Kumar<sup>3</sup> |  
 Devendra Singh Negi<sup>4</sup> | Indra Bahadur<sup>5</sup> 

<sup>1</sup>Department of Chemistry, Maharishi Markandeshwar (Deemed to be University), Haryana, India

<sup>2</sup>Department of Chemistry, Himachal Pradesh University, Shimla, India

<sup>3</sup>Department of Chemistry, SGRR (PG) College, Dehradun, India

<sup>4</sup>Department of Chemistry, H. N. B. Garhwal University, Srinagar, India

<sup>5</sup>Department of Chemistry, Faculty of Natural and Agricultural Sciences, North-West University, South Africa

## Correspondence

Gunjan Chauhan, Department of Chemistry, Maharishi Markandeshwar (Deemed to be University), Haryana 133207, India.

Email: [gunjan.ch.86@gmail.com](mailto:gunjan.ch.86@gmail.com)

Indra Bahadur, Department of Chemistry, Faculty of Natural and Agricultural Sciences, North-West University, South Africa.

Email: [bahadur.indra@nwu.ac.za](mailto:bahadur.indra@nwu.ac.za)

## Abstract

CoS@MorphcdtH NPs and CoS@4-MPipzcdtH NPs were synthesized by precipitation method involving three mechanisms: inclusion, occlusion, and adsorption. The synthesized NPs were characterized with the help of UV-Vis spectroscopy, FESEM-EDAX, powder x-ray diffraction, TEM, ESIMS, TG/DSC analysis. The morphology of the CoS@MorphcdtH NPs and CoS@4-MPipzcdtH NPs were hexagonal and rectangular, and the particles were in the range 7–12 nm. UV-visible spectral measurements showed surface plasmon resonance at 320 nm–340 nm with band gap of 3.65 eV–3.86 eV. The catalytically active CoSNPs called were investigated for the reduction of 4-nitrophenol (4-NP) via hydrogenation using sodium borohydride (NaBH<sub>4</sub>) as a reducing agent. Both the CoS NPs successfully reduced 4-NP to 4-aminophenol (4-AP) in a short time, catalytic performances are almost unchanged for the first five cycles. Herein, we report the preparation and characterizations of efficient active CoS NPs consisting carbodithioic acid framework as a support/capping material, along with catalytic property.

## KEYWORDS

catalytic route, CoS NPs, rate constant, reducing agent, support material

## 1 | INTRODUCTION

4-NP(4-nitrophenol) is a highly hazardous pollutant and potentially toxic to living organisms.<sup>[1,2]</sup> The potential cause of cyanosis is methemoglobinemia, which is due to the delayed interaction of 4-NP with blood. It causes vomiting and abdominal pain, while prolonged contact with the skin results in an allergic response; therefore, 4-NP appeared to be poisonous, anthropogenic, and inhibitory by nature.<sup>[3]</sup> Symptoms such as drowsiness,

nausea, and headache appeared due to the short-term exposure through the pathways of inhalation and ingestion whereas getting in contact with the eyes results in irritation.<sup>[4]</sup> Dosage, time, passageway, gender, nutritional status, lifestyle, family traits, etc., are the parameters on which the severity of human health depends when comes in contact with 4-NP. 4-NP is one of the most virulent derivatives of the parathion insecticide and is mutagenic, cytotoxic, embryo-toxic, and carcinogenic by nature.<sup>[5]</sup>

This is an open access article under the terms of the [Creative Commons Attribution](https://creativecommons.org/licenses/by/4.0/) License, which permits use, distribution and reproduction in any medium, provided the original work is properly cited.

© 2023 The Authors. *Journal of the Chinese Chemical Society* published by Chemical Society Located in Taipei and Wiley-VCH GmbH.

4-NP resist bio-degradation, is known to be highly stable and soluble in the freshwater, marine environment, and wastewaters, and is found to be present as pollutants in industrial effluents. Researchers have developed many techniques for the eradication, including adsorption, electrocoagulation, electrochemical treatment, microbial degradation, photocatalytic degradation, electro-Fenton, and catalytic oxidation facilitated by the microwave method etc.<sup>[6–10]</sup> However, all these techniques are not very effective and even energy-consuming. Using reductive conversion of a lethal chemical 4-NP to a more biodegradable 4-AP (aminophenol) is another efficient solution. The reduction from 4-NP to 4-AP has great commercial importance as 4-AP is a valuable chemical for producing drugs (analgesic, antipyretic) and has also been used indifferent applications such as corrosion inhibitor, hair-dyeing agent, and photographic developer.<sup>[11]</sup> Many methods, such as homogeneous/heterogeneous catalytic reduction, electrolytic reduction, metal-acid reduction, and direct catalytic reduction reactions, are used for the transformation of 4-AP from 4-NP.<sup>[12]</sup> Among them, the catalytic reduction route minimizes the effluent disposal problems to a great extent as it represents a greener and more effective technology and improves product quality with the overall process economy.<sup>[13]</sup> The reduction 4-NP in the presence of nanoparticles (NPs) with NaBH<sub>4</sub> as a reducing agent into 4-AP is a recent technology.<sup>[14–18]</sup> There are various routes for synthesizing nanoparticles, such as physical, chemical, and biological. The biosynthesis pathway is considered a greener approach, and plants, microorganisms, and biomolecules have been used for the preparation of various nanoparticles.<sup>[19,20]</sup>

The present work proposes the fabrication of CoS@MorphcdtH NPs and CoS@4-MPipzcdtH NPs via simple and cost-effective chemical precipitation method. Dithiocarbamate complexes as a supporting/capping materials are normally more secure, less expensive, and steadier than the utilization of other precursors. In addition, the appropriate changes in the natural moiety of dithiocarbamate complex can affect the phase, size, shape, and physical–chemical properties of the metal sulfide nanoparticles, which are well documented in the literature.<sup>[21–23]</sup> The advantage of using MorphcdtH and 4-MPipzcdtH as support/capping material is to prevent agglomeration, stabilizing metal nanoparticles, and maintain their finely dispersed state. Support materials MorphcdtH and 4-MPipzcdtH add complexity to final catalytic systems by transferring charge to and/or from the surface of metal nanocrystals, also creating noncovalent interactions with the reactant used in a catalytic reduction. The detailed characterizations of well crystalline CoS@MorphcdtH NPs and CoS@4-MPipzcdtH NPs

have been reported which offered complete and precise information about the nanoparticles. In this report, we also have shown the application of the CoS@MorphcdtH NPs and CoS@4-MPipzcdtH NPs for the catalytic reduction of nitrophenol group. The reaction between CoS@MorphcdtH NPs and CoS@4-MPipzcdtH NPs has many advantages, including (i) conversion into chemo/regio selective product (ii) reaction is used for the reduction of nitrophenol (iii) multiple time usage of without degradation in its activity.

## 2 | EXPERIMENTAL SECTION

### 2.1 | Materials

All the chemicals and the solvents used for this experiment were listed as: ethanol, methanol, toluene, carbon disulfide, 1-methylpiperazine, morpholine, dimethylsulfoxide, sodium sulfide, cobalt acetate tetrahydrate, sodium borohydride, and 4-Nitrophenol. All were of analytical purity and further used as obtained from Merck. All glassware used during the experiment was cleaned in freshly prepared chromic acid/aqua regia solution and rinsed thoroughly with deionized water.

### 2.2 | Preparation of support/capping material

Reviewing the literature,<sup>[24]</sup> a CS<sub>2</sub> group has been introduced to fabricate 4-methylpiperazine-1-carbodithioic acid and morpholinecarbodithioic acid (MorphcdtH) using the N–H bond of heterocyclic amines. Free carbodithioic acids exist in zwitterionic form and have high stability because of higher lattice energy effects.

#### 2.2.1 | MorphcdtH (C<sub>5</sub>H<sub>9</sub>ONS<sub>2</sub>; white)

Analysis found: C-36.76, H-5.52, N-8.51, S-39.24%; Yield 98%. Decomposition Temperature: 185°C. FTIR (KBr) cm<sup>-1</sup>: (OH) 3,540–3,250 b,s, 1449, a(SCS) 985, s(SCS) 671.

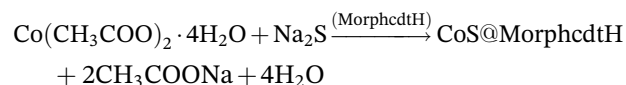
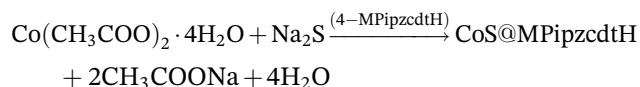
#### 2.2.2 | 4-MPipzcdtH (C<sub>6</sub>H<sub>12</sub>N<sub>2</sub>S<sub>2</sub>; Creamish yellow)

Analysis found: C - 40.93, H- 6.02, N- 15.60, S- 35.90%; Yield 99%. Decomposition temperature: 200°C. FTIR (KBr) cm<sup>-1</sup>: (N-H) 3,600–3,200 b,s, (C-H)/(N-CH<sub>3</sub>) 2850 s, 1442 s, a(SCS) 975 s, s(SCS) 675 w.

## 2.3 | Synthesis of CoSNPs

In a typical experiment, 0.1308 g of MorphcdtH and 0.1411 g of MPipzcdtH dissolved in methanol (3 mL) were added to the 0.100 g continuously stirred solution of  $\text{Co}(\text{CH}_3\text{COO})_2 \cdot 4\text{H}_2\text{O}$ . The reaction mixture was stirred for 3–5 minutes until homogeneity was obtained. Methanolic solution (3 mL) of  $\text{Na}_2\text{S}$  (0.0938 g; 1.203 mmol) was added slowly to continuously stirred homogeneous solution. Green precipitates of  $\text{CoS@MorphcdtH}$  NPs and  $\text{CoS@4-MPipzcdtH}$  NPs were obtained after another 2 hours continuous stirring, respectively. The resultant nanoparticles of  $\text{CoS@MorphcdtH}$  and  $\text{CoS@4-MPipzcdtH}$  were collected by centrifugation technique, washed several times with methanol, and dried overnight by keeping in  $\text{CaCl}_2$  desiccator. The reaction for the

synthesis can be expressed according to equations given below:



### 2.3.1 | [ $\text{CoS@MorphcdtH}$ ; ( $\text{CoC}_{10}\text{H}_{18}\text{N}_2\text{S}_5\text{O}_2 = 416.95$ )] green

Analysis Found: Co-13.95%, S-38.14%; Calculated: Co-14.13%, S-38.37%, Yield 99%. Decomposition temperature: 260°C.

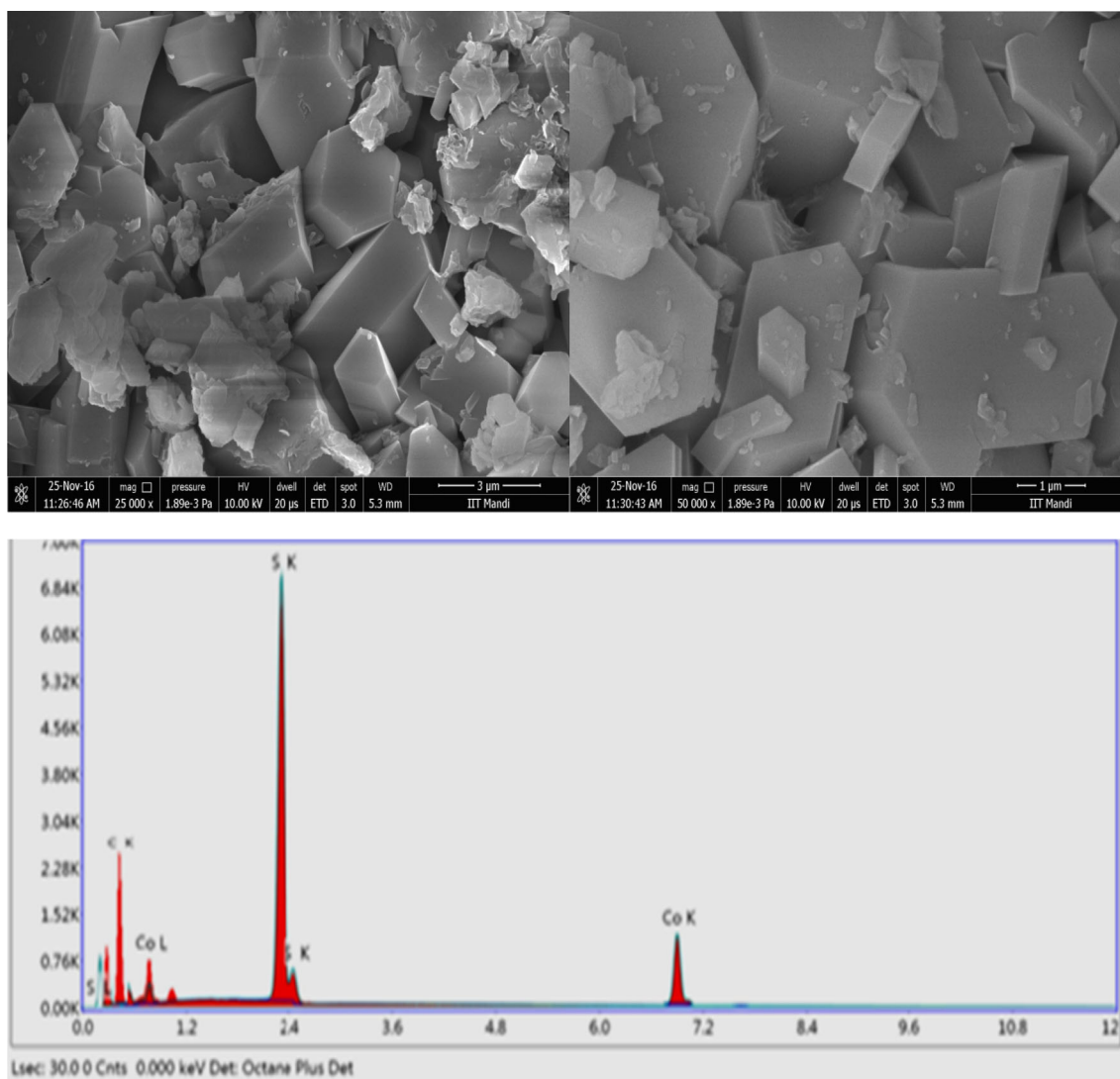


FIGURE 1 FESEM images and EDAX spectrum of  $\text{CoS@4-MPipzcdtH}$  NPs.

### 2.3.2 | [CoS@MPipzcdtH]; (CoC<sub>12</sub>H<sub>24</sub>N<sub>4</sub>S<sub>5</sub> = 442.93) green

Analysis Found: Co-13.10%, S-36.05%; Calculated: Co-13.30%, S-36.12%, Yield 99%. Decomposition temperature: 310°C.

## 2.4 | Detection method

SU8010 was used to determine the morphology and elemental composition of both samples and details about the instruments and method were found elsewhere.<sup>[25]</sup> The crystalline nature of CoS NPs was analyzed using a powder x-ray diffraction (PXRD) method on a XPERT-PRO x-ray diffractometer operating at the voltage of

45 kV, the current of 40 mA with CuK $\alpha$  radiation at the wavelength of 1.5406 nm and step size of 0.050 per sec counting in the range  $2\theta$  from 10° to 80°. The range of the UV-visible spectrophotometer was 900–200 nm, methanol was used as a reference and the surface spectrum of CoS NPs was measured. Thermal analysis of samples was carried and details about it were found elsewhere.<sup>[25]</sup>

## 2.5 | Catalytic activity

The catalytic performance of CoS NPs has been performed in relation to the change in the initial concentration of 4-NP to 4-AP and the complete conversion was detected at the time when the yellow color of the mixture

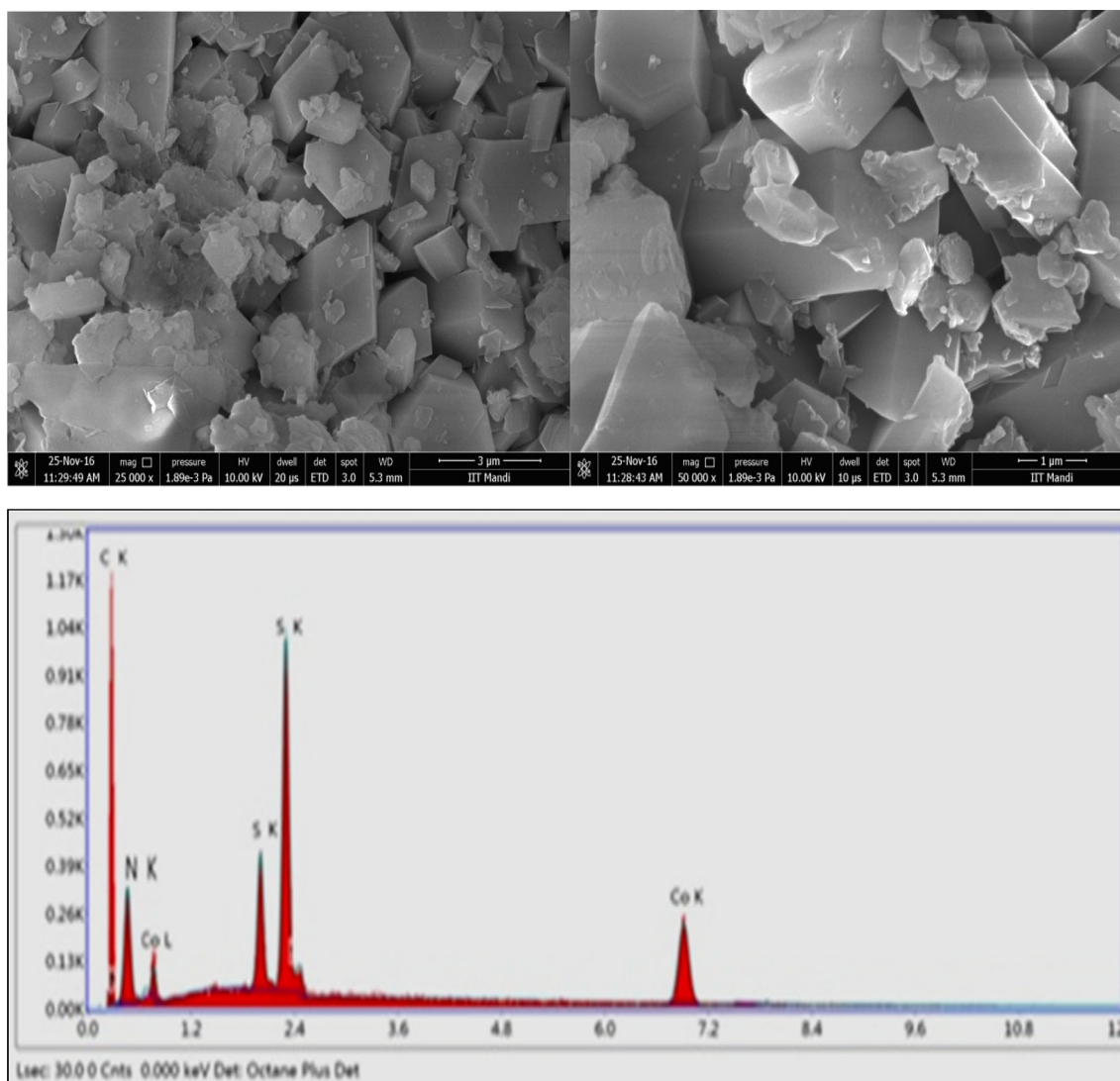


FIGURE 2 FESEM images and EDAX spectrum of CoS@MorphcdtH NPs.

turns into a faded yellow-green color. The catalytic behavior was analyzed at a concentration of 0.004 g of CoS@MorphcdtH NPs and 0.005 g of CoS@4-MPipzcdtH NPs per 1 mL of  $10^{-4}$  M aqueous solution. 10 mL of the freshly prepared aqueous solution of  $\text{NaBH}_4$  (0.30 mL; 15 mM) was introduced in 100 mL of 4-NP (3.0 mL, 0.15 mM) at room temperature. It was further treated with CoS@MorphcdtH NPs and CoS@4-MPipzcdtH NPs at different time intervals. After the addition of a trace amount of the CoS@MorphcdtH NPs and CoS@4-MPipzcdtH NPs indicate the formation of a new band at 300 nm. Reduction and formation of the 4-NP and 4-AP indicate the increased intensity. The progress of a reaction is monitored by using UV-visible spectrophotometry.

### 3 | RESULTS AND DISCUSSION

The surface morphology of the CoS@MorphcdtH NPs and CoS@4-MPipzcdtH NPs showed hexagon shapes were illustrated in Figures 1 and 2, respectively. Energy Dispersive x-ray spectroscopy was used to confirm the

elemental composition. The homogeneity of capping agents was observed at the top layer of the sample, which indicates that uniform distribution was achieved during fabrication. The EDAX spectrum confirmed the elemental composition as wt. %: CoS@MorphcdtH NPs gave cobalt, sulfur, nitrogen, and carbon of 51.45, 39.20, 2.01, and 5.96, respectively whereas 53.14, 41.89, 1.45, and 3.06 for CoS@4-MPipzcdtH NPs.

Typical TEM micrographs of CoS@MorphcdtH NPs and CoS@4-MPipzcdtH NPs exhibited hexagonal and rectangle shapes respectively. The average particle size which falling in the range 7–12 nm in diameter follows the increasing order as CoS@MorphcdtH NPs < CoS@4-MPipzcdtH NPs. Critical investigation of the average particle size of CoS@MorphcdtH NPs and CoS@4-MPipzcdtH NPs deduces that core diameter changes with the increase/decrease of carbon chain length at the fourth position in the heterocyclic ring of carbodithioic acid as capping agents. The capping agent is used in excess stoichiometric amounts than required, resulting in the aggregation of the smaller particles to form markedly larger nonspherical particles which are most possibly due to some overlapped

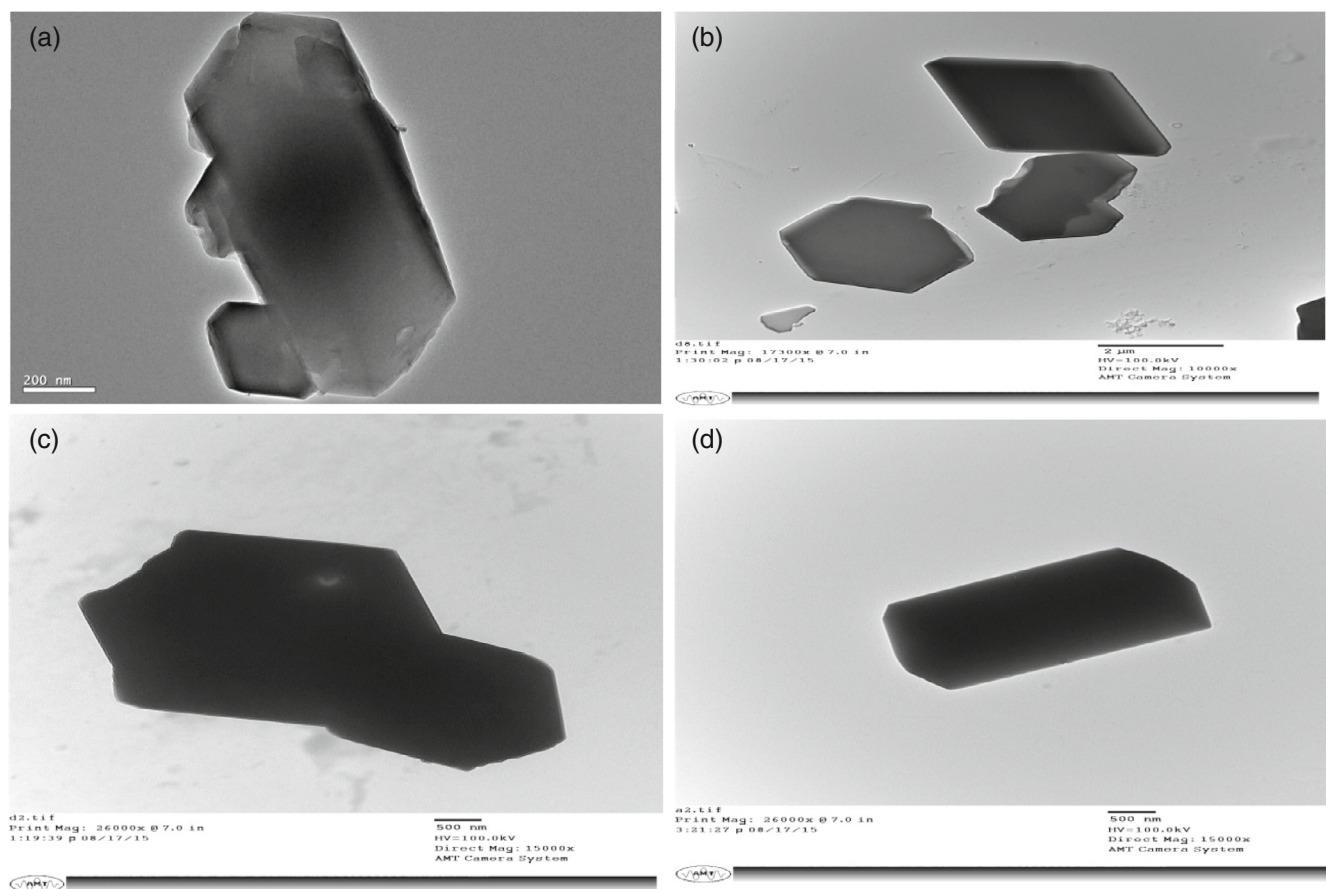
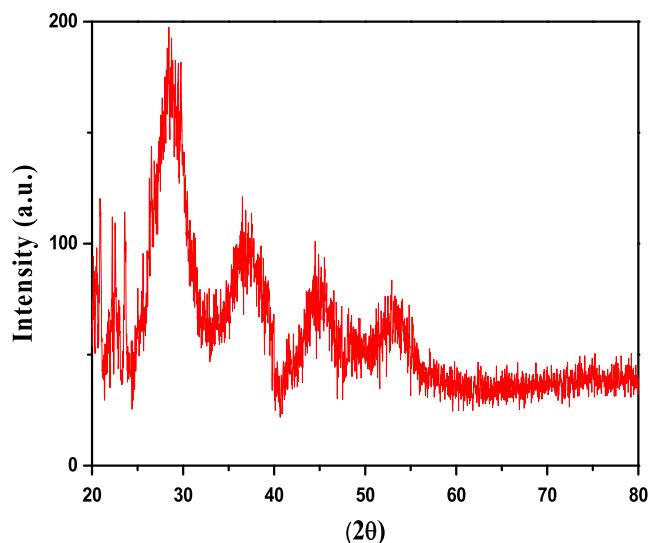


FIGURE 3 TEM micrographs of (a), (b) CoS@MorphcdtH NPs and (c), (d) CoS@4-MPipzcdtH NPs.

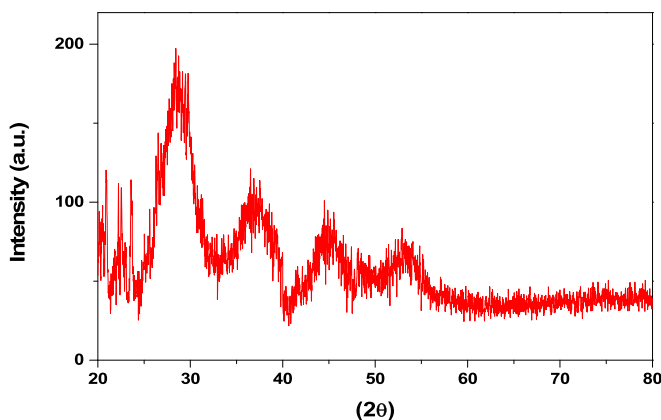
lattice effects of the capping agent (Figure 3). Observation in terms of morphology is in consonance with FESEM study.

Diffraction patterns of CoS@MorphcdtH NPs and CoS@4-MPipzcdtH NPs exhibited four peaks at nearly same  $2\theta$  and d-spacing values irrespective of nature of capping



2 Theta (°)	d-spacing (Å)	FWHM (°)	Dp (nm)	Lattice constant (a)	Lattice constant (c)
28.72	2.9245	1.2055	7.11	3.377	5.14
36.51	2.5394	1.2141	7.20	3.377	5.12
47.22	1.9260	1.2241	7.40	3.376	5.12
56.21	1.688	1.1914	7.90	3.376	5.11

FIGURE 4 PXRD patterns and data of CoS@MorphcdtH NPs.



2 Theta (°)	d-spacing (Å)	FWHM (°)	Dp (nm)	Lattice constant (a)	Lattice constant (c)
29.39	2.9245	0.7786	11.02	3.377	5.15
36.22	2.5425	0.7596	11.5	3.376	5.15
46.15	1.9300	0.7651	11.8	3.375	5.14
56.75	1.6875	0.7831	12.05	3.375	5.14

FIGURE 5 PXRD patterns and data of CoS@4-MPipzcdtH NPs.

agents. CoS@MorphcdtH NPs and CoS@4-MPipzcdtH NPs showed in range: (a)  $28.72^\circ - 29.39^\circ$ , (b)  $36.22^\circ - 36.51^\circ$ , (c)  $46.15^\circ - 47.22^\circ$ , and (d)  $56.21^\circ - 56.75^\circ$  as shown in Figures 4 and 5. The position of Bragg's bands for CoS@MorphcdtH NPs and CoS@4-MPipzcdtH NPs corresponds to the above  $2\theta$  values, indexed in the (100), (101), (102), and (110) crystal planes respectively.<sup>[26,27]</sup> For the hexagonal structure of cobalt sulfide, the  $2\theta$  values and their corresponding d-spacing values match well with the standard JCPDS card number - 65-3418. The average crystallite size evaluated using Debye - Scherrer equation<sup>[28]</sup> falls in the range of 7.11 nm-12.05 nm for CoS@MorphcdtH NPs and CoS@4-MPipzcdtH NPs. The nature of capping agents and their effect on crystal lattice has further been studied by computing lattice constant. The lattice constant 'a' and 'c' for CoS@MorphcdtH NPs and CoS@4-MPipzcdtH NPs falls within the range 3.375–3.377 and 5.11–5.15, respectively. CoS@MorphcdtH NPs and CoS@4-MPipzcdtHNPs were synthesized by precipitation method involving three mechanisms: inclusion, occlusion, and adsorption. The catalytically active CoS nanoparticles (NPs) called were investigated for the reduction of 4-nitrophenol (4-NP) via hydrogenation using sodium borohydride ( $\text{NaBH}_4$ ) as a reducing agent. Both the CoSNPs successfully reduced 4-NP to 4-aminophenol (4-AP) in a short time and could be used for more than five times without obvious fading in their catalytic activities. Herein, we report the preparation and characterizations of efficient active CoS NPs consisting carbodithioic acid framework as a support/capping material, along with catalytic properties.

SPR spectra of CoS@MorphcdtH NPs and CoS@4-MPipzcdtH NPs depict the existence of peaks at 320 nm and 340 nm respectively. Observation of SPR bands in a particular range of wavelength in nm followed the increasing order with respect to the size of the heterocyclic group of a capping agent. Based on the steric interactions of these groups, the trend well matched with the size of nanoparticles as evident from TEM studies. UV-visible absorption of CoS@MorphcdtH NPs and CoS@4-MPipzcdtH NPs exhibited broad peaks which were blue-shifted as compared with bulk CoS.<sup>[25,29,30]</sup> Slight variation in broadness and positions of peaks from bulk to CoS@MorphcdtH NPs and CoS@4-MPipzcdtH NPs (Figure 6) may be because of the absorptions of capping agents. The band gaps in the present study were found to be 3.86 eV and 3.65 eV for CoS@MorphcdtH NPs and CoS@4-MPipzcdtH NPs, respectively.

ESI-MS pattern of CoS@4-MPipzcdtH NPs displayed a peak at  $m/z = 442.93$  corresponding to its molecular mass and intense peak at  $m/z = 124.93$  (93%) which is assigned to the  $[\text{CoS}_2]^+$  ion. The peaks due to ion fragments  $\{\text{CoS}(\text{NHCH}_2\text{CH}_2\text{CH}_2\text{CH}_2\text{N}[\text{CS}_2])_2\}^+$ ,  $\{\text{CoS}.$

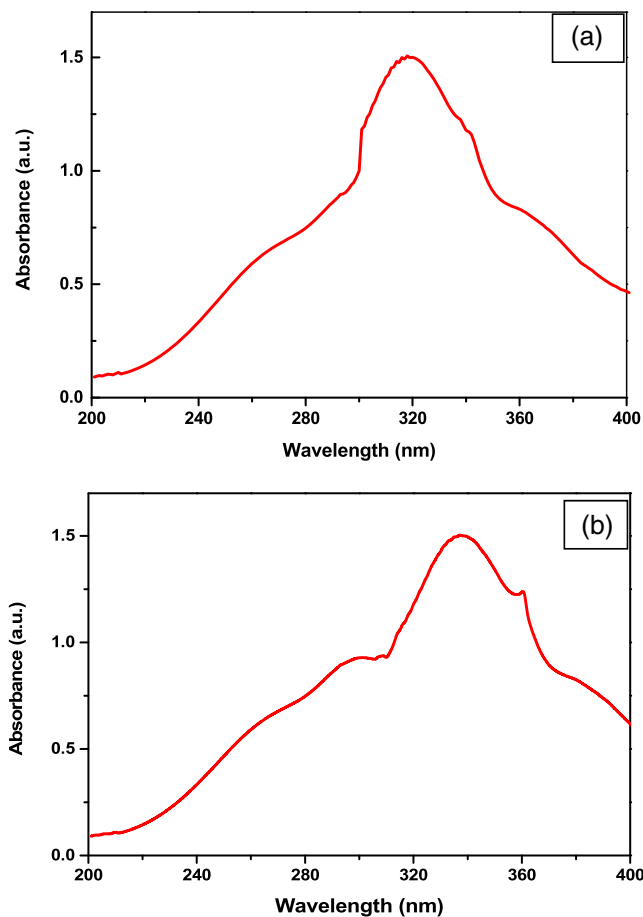


FIGURE 6 Electronic absorption spectrum of (a) CoS@MorphcdtH NPs and (b) CoS@4-MPipzcdtH NPs.

$(\text{CH}_2\text{CHN}(\text{CS}_2))_2\}^+$ ,  $\{\text{CoS}(\text{NH}(\text{CS}_2))_2\}^+$ ,  $\{\text{CoS}(\text{CS}_2)_2\}^+$ ,  $\{\text{CoS}(\text{CS}_2)\}^+$ , and  $[\text{CoS}_2]^+$  appeared at  $m/z$  412.93 (25%); 326.93 (13%), 274.93 (19%); 244.93 (15%), 168.93 (19%), and 124.93 (93%) respectively. The proposed fragmentation mechanism (Figures 7 and 8) is in agreement with the ring-opening mechanism of cyclic amines which involves the cleavage of the bond next to the nitrogen atom.<sup>[25]</sup>

TG/DSC curves of CoS@MorphcdtH NPs revealed the IDT, decomposition range, and exotherm at temperature of  $115^\circ\text{C}$ ,  $270-280^\circ\text{C}$ , and  $318^\circ\text{C}$  whereas for CoS@4-MPipzcdtH NPs these were observed at  $120^\circ\text{C}$ ,  $310^\circ\text{C}$ , and  $320^\circ\text{C}$  respectively. The TG/DSC curve of CoS@MorphcdtH NPs and CoS@4-MPipzcdtH NPs exhibits two steps decomposition as shown in Figures 9 and 10. For CoS@MorphcdtH NPs, an initial mass loss of 4.33% in the temperature range  $110-140^\circ\text{C}$  corresponds to the loss of one mole of water, the subsequent mass loss of 78.37% in the temperature range  $260-310^\circ\text{C}$  has been proposed to be the oxidative decomposition of two moles of morpholinecarbodithioic acid ( $\text{C}_5\text{H}_9\text{ONS}_2$ ) to give CoO as final product. The nature of end products was complimented by measuring the PXRD of residues. It was found

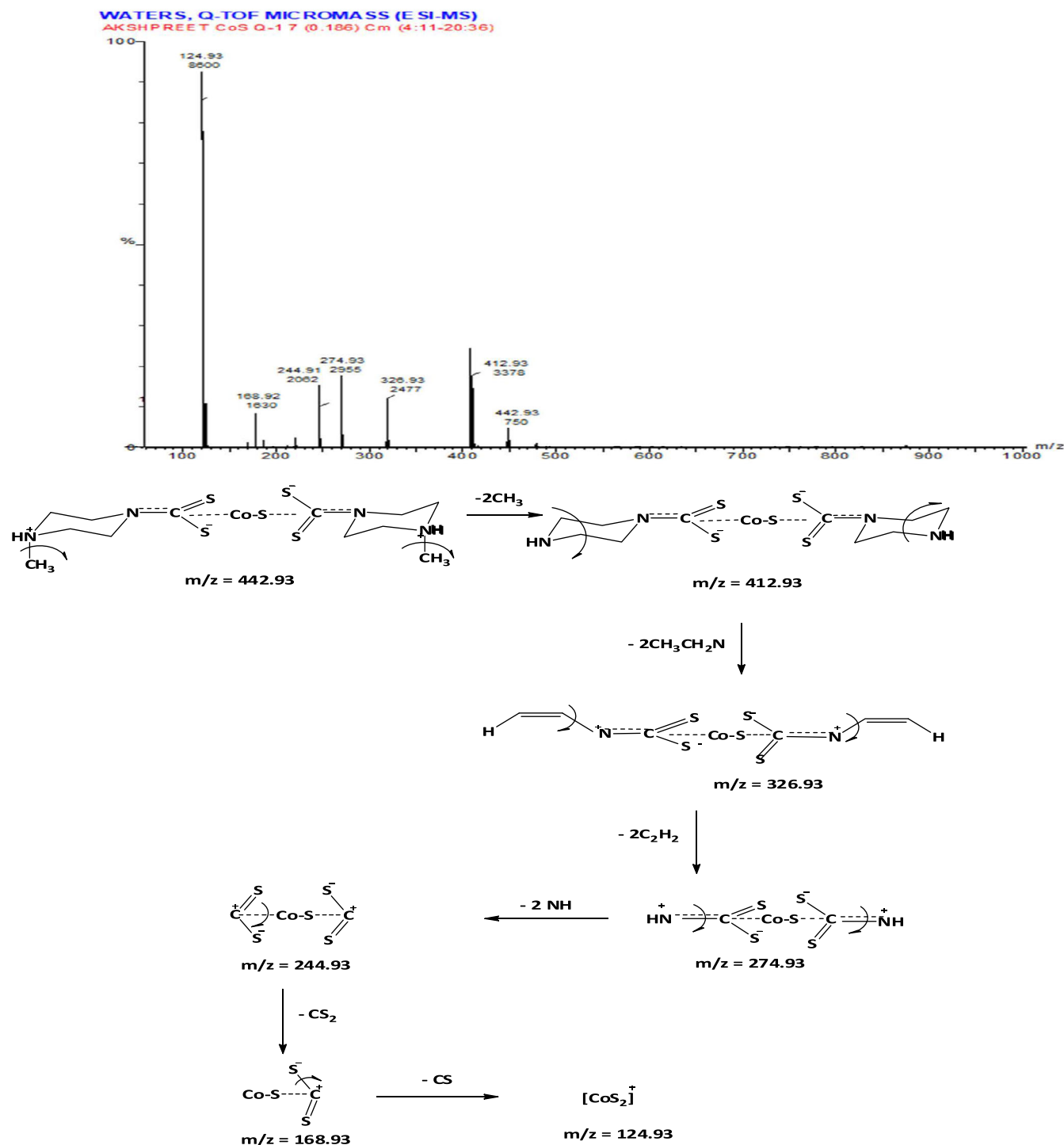


FIGURE 7 Mass spectrum and Proposed Fragmentation pattern of CoS@4-MPipzcdtH NPs.

that CoO is the final product which is stable for temperatures up to 800°C.

### 3.1 | PXRD of TG residues

The composition of final product was determined by using powder x-ray diffraction technique. For

this the residues of CoS@MorphcdtH NPs and CoS@4-MPipzcdtH NPs obtained from TG study had been used. The  $2\theta$  values 37.89°, 42.55°, 61.27°, 73.19°, and 75.32° of TG residues of CoS NPs correspond to the crystal planes 111, 200, 220, 311, and 222 respectively. PXRD pattern of residues of CoS NPs matches well with rock-salt structure of CoO with JCPDS card no. 431004.<sup>[31]</sup> The diffraction peaks were not observed

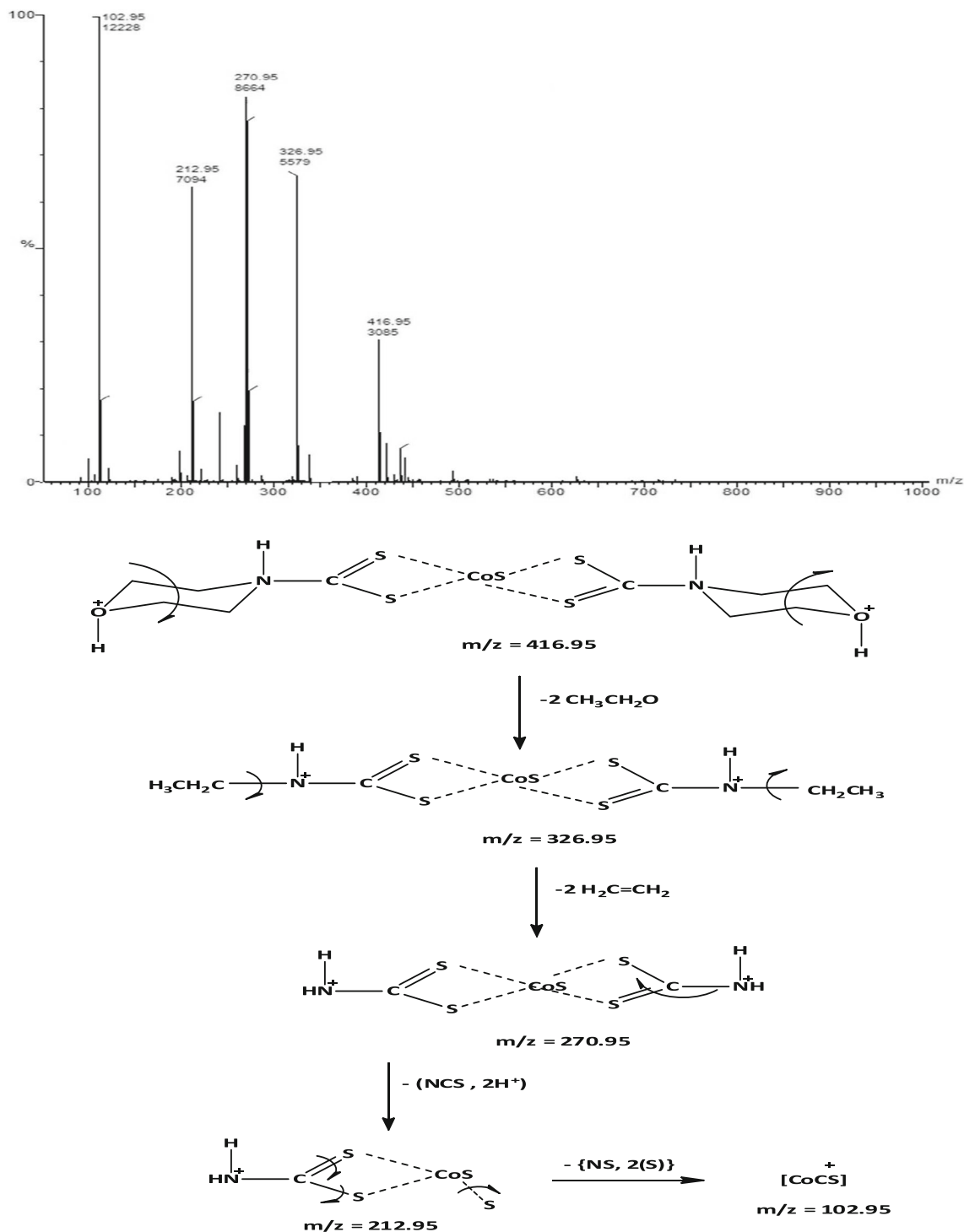


FIGURE 8 Mass spectrum and Proposed Fragmentation pattern of CoS@MorphcdtH NPs.

for metallic Co or  $\text{Co}_3\text{O}_4$ . Thus the observed PXRD patterns (Figures 11 and 12) of TG residues confirmed the CoO as final decomposition product and hence is in agreement with the proposed decomposition pathway.<sup>[25]</sup>

### 3.2 | Catalytic reduction of 4-nitrophenol

Langmuir-Hinshelwood mechanism for the reduction of 4-NP became the efficient and prevalent route.<sup>[32,33]</sup> The peculiar catalytic activity depends on the small

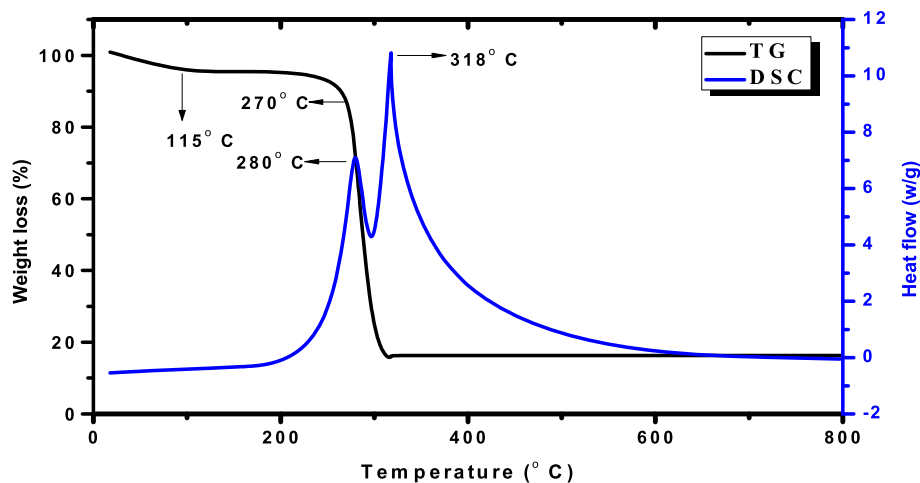


FIGURE 9 TG/DSC curves of CoS@MorphcdtH NPs.

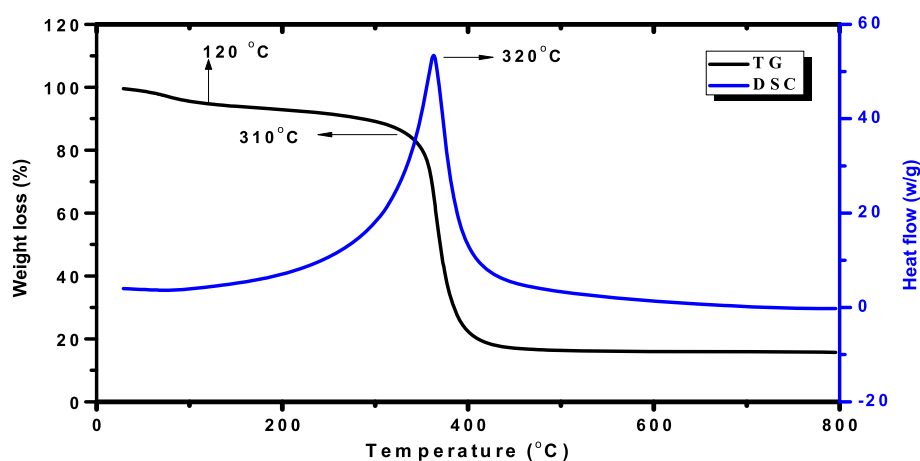


FIGURE 10 TG/DSC curves of CoS@4-MPipzcdtH NPs.

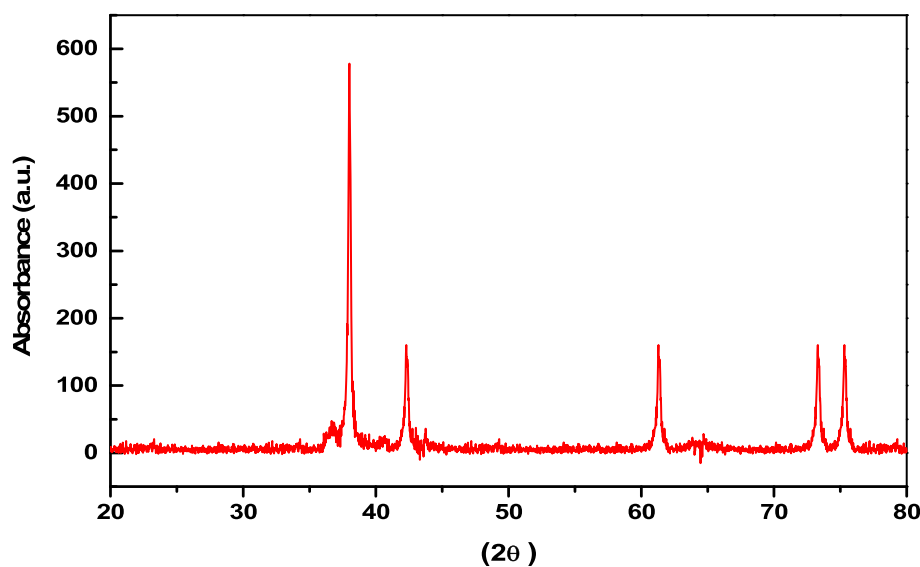


FIGURE 11 PXRD of TG residue of CoS@MorphcdtHNPs.

size of the NPs, mostly they have higher catalytic activity.

The surface of NPs serves as the active location where the process of catalytic reduction occurs and the nanoparticles remains active even at room temperature.

Borohydride ions bind to the surface whereas alongside 4-NP also adsorbs on the nanocatalyst surface. Subsequently, 4-NP is reduced by borohydride ions to 4-AP which is a rate-determining step. 4-NP exhibits light yellow color and display a strong absorption band at

FIGURE 12 PXRD of TG residue of CoS@4-MPipzcdtH NPs.

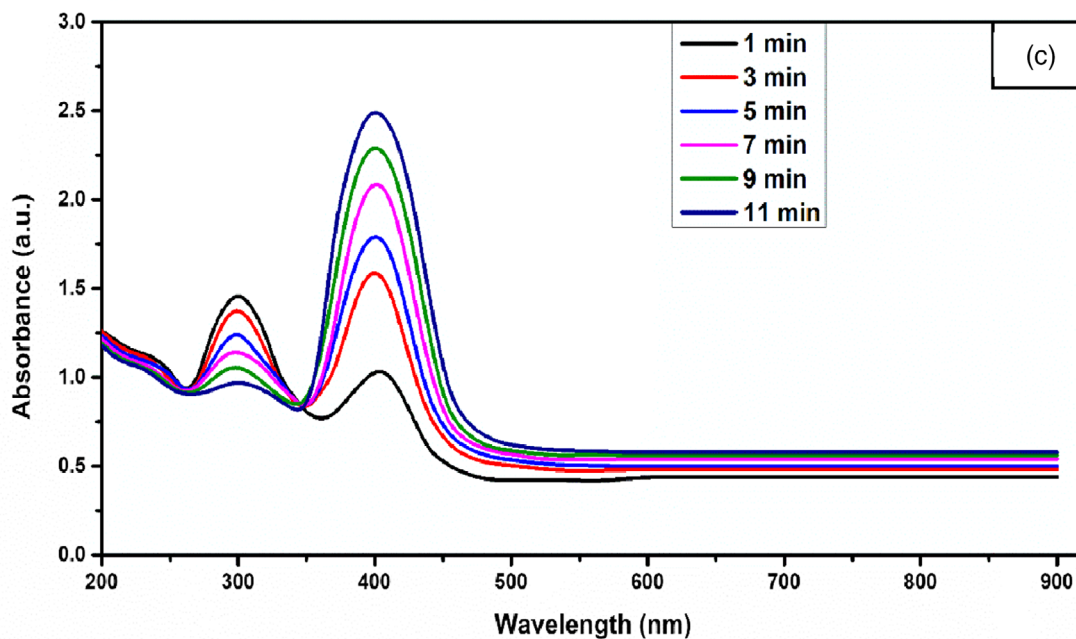
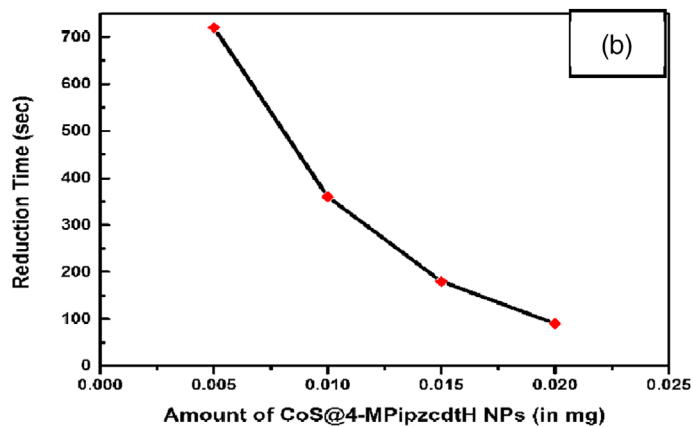
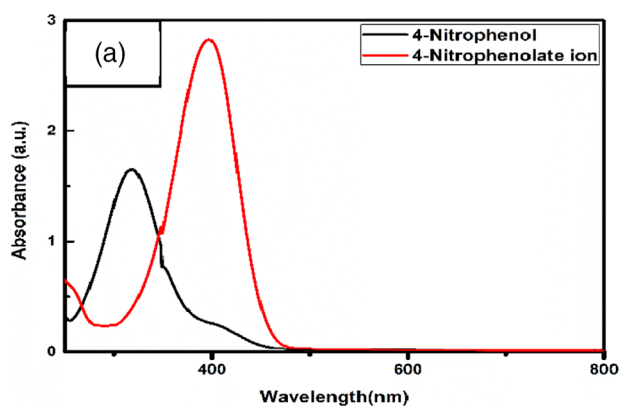
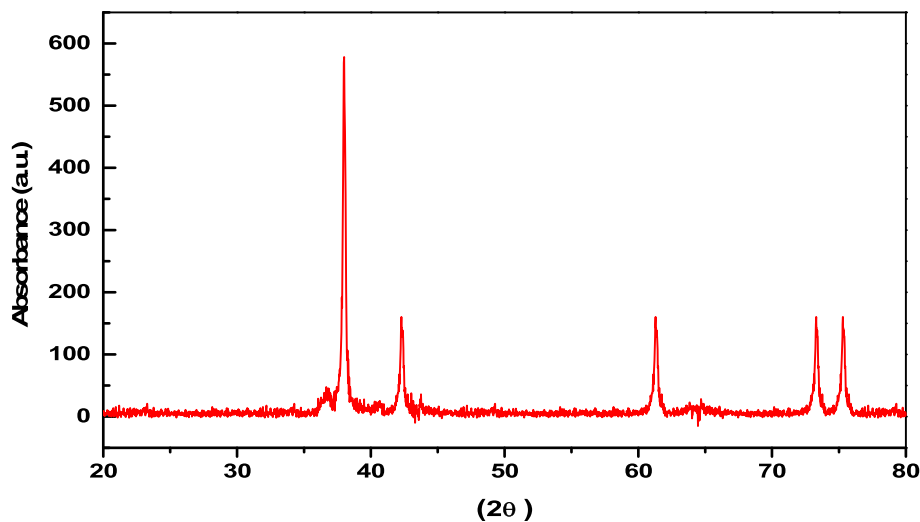


FIGURE 13 (a) UV-visible spectra of 4-NP before and after addition of NaBH<sub>4</sub> solution; (b) effect of CoS@4-MPipzcdtH NPs amount in the reduction of 4NP - 4AP; (c) 4-NP with NaBH<sub>4</sub> in the presence of CoS@MorphcdtHNPs as catalyst at room temperature.

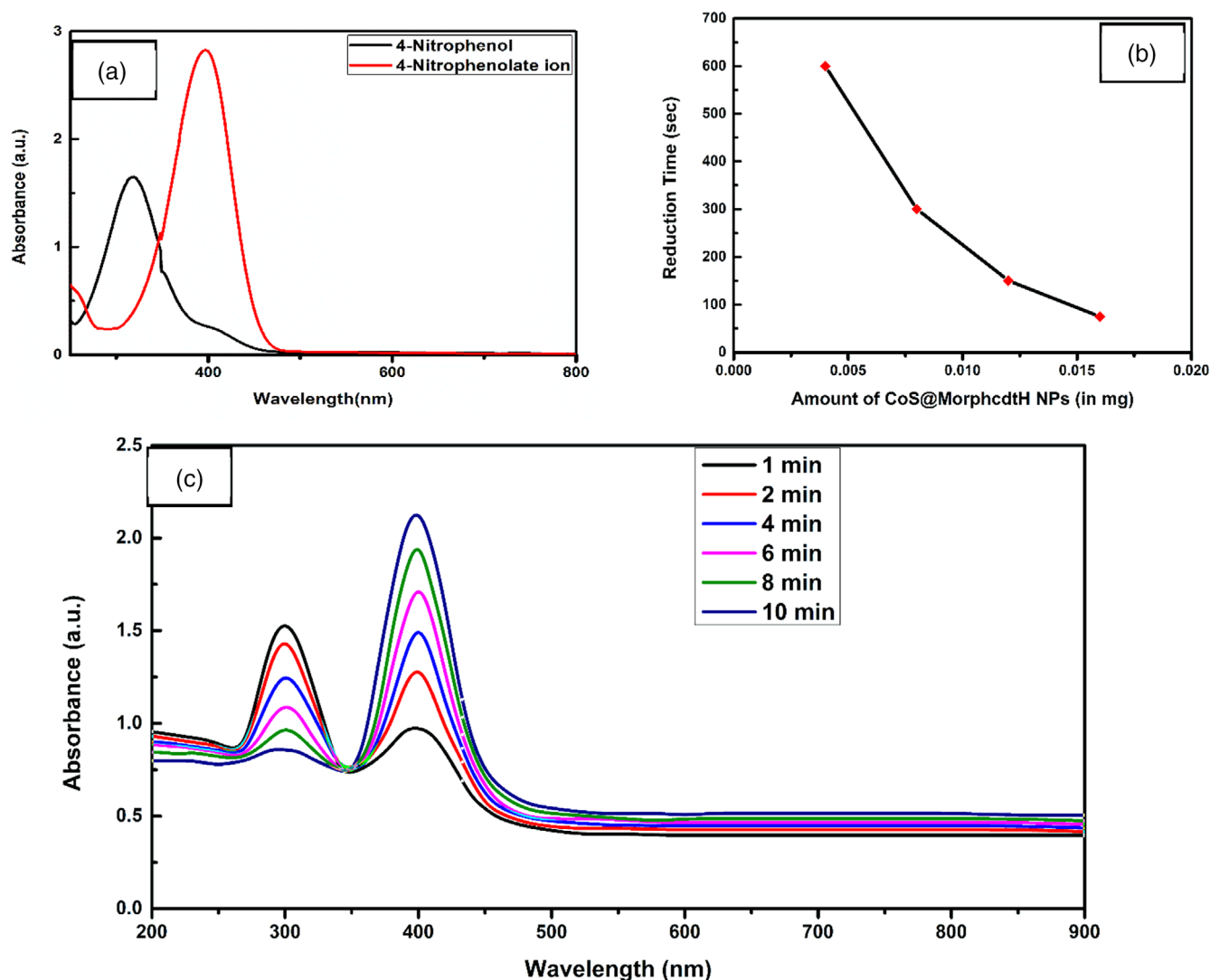


FIGURE 14 (a) UV-visible spectra of 4-NP before and after addition of  $\text{NaBH}_4$  solution; (b) effect of  $\text{CoS@MorphcdtH}$  NPs amount in the reduction of 4NP-4AP; (c) 4-NP with  $\text{NaBH}_4$  in the presence of  $\text{CoS@4-MPipzcdtH}$  NPs as catalyst at room temperature.

TABLE 1 Comparison of rate constants of catalytic reaction in the presence of  $\text{CoS@MorphcdtH}$  and  $\text{CoS@4-MPipzcdtH}$  catalysts.

Catalyst	Morphology	Target compound	Catalyst dose	Degradation rate	Reusability
$\text{CoS@MorphcdtH}$	~ 8 nm	4- NP	0.004 g	$0.183 \text{ min}^{-1}$	Five
$\text{CoS@4-MPipzcdtH}$	~ 12 nm	4- NP	0.005 g	$0.189 \text{ min}^{-1}$	Five

317 nm. Upon the addition of  $\text{NaBH}_4$  to solution leads to a distinct color change (light to intense yellow) due to formation of 4-nitrophenolate ion as shown in Figures 13a and 14a. Color change results in alteration in the pH, that is, acidic to highly basic leading to an immediate shifting in absorption peak of 4-NP from 317 nm to 400 nm because of the formation of 4-nitrophenolate ion.<sup>[15,17,34–39]</sup>

Furthermore, the absorption intensity remains almost unchanged even after standing for 2 hours which clearly

suggesting that the reduction did not proceed in the absence of the catalyst. With the addition of  $\text{CoS@MorphcdtH}$  NPs and  $\text{CoS@4-MPipzcdtH}$  NPs into the reaction system led to emergence of gradually decrease in absorption intensity of 4-NP. The formation of 4-AP in a basic medium at room temperature<sup>[39]</sup> indicated by the appearance of a new absorption peak at 300 nm. The reduction reaction completed within 11 min for  $\text{CoS@4-MPipzcdtH}$  NPs and 10 min for  $\text{CoS@MorphcdtH}$  NPs which is evidenced by fading of the

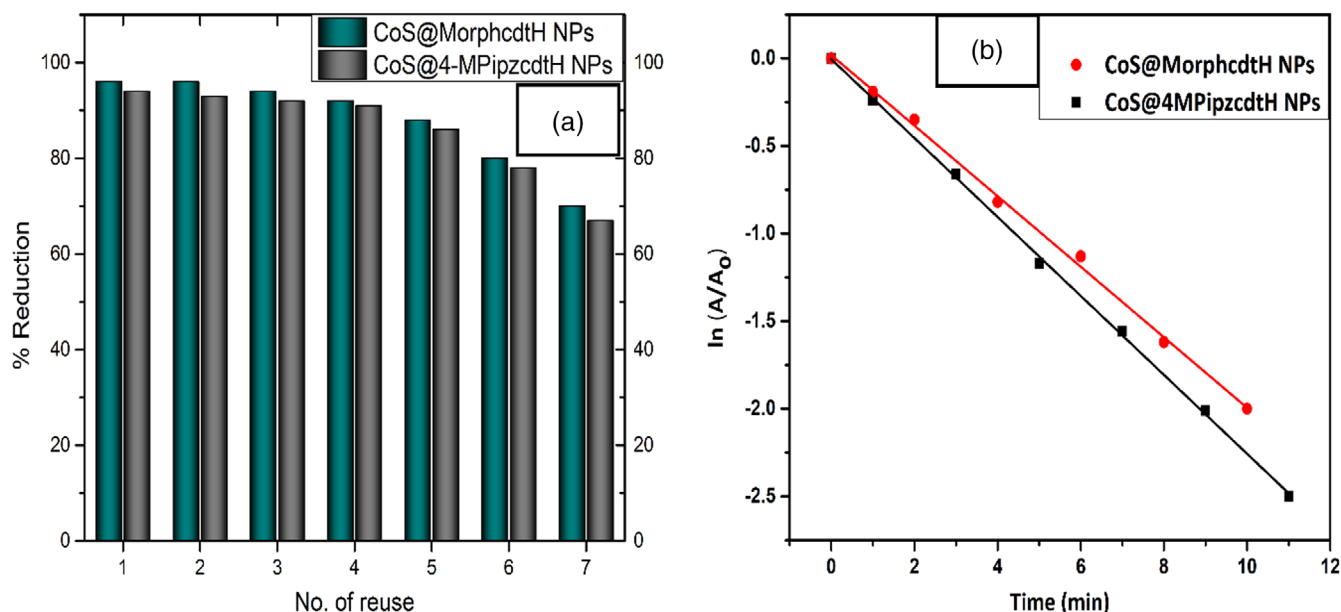


**FIGURE 15** Reusable performance of (a) CoS@MorphcdtH NPs, (b) CoS@4-MPipzcdtH NPs as a catalyst for consecutive cycles and pseudo-first order kinetic plot ( $\ln(A/A_0)$ ) versus time for the catalytic reduction of 4-NP.

yellow-green color of the reaction solution (Figures 13 and 14). The concentration of  $\text{NaBH}_4$  is in large excess to that of 4-NP, the reduction considered as a pseudo first-order reaction with regard to 4-NP (Table 1).

The reaction kinetics are given by  $\ln(A/A_0) = -kt$ , where  $t$  denotes the reaction time,  $k$  is first-order rate constant ( $\text{min}^{-1}$ ). The concentrations of 4-NP at time  $t$  and 0 are denoted by  $A$  and  $A_0$  respectively. A linear relationship between  $\ln(A/A_0)$  and reaction time  $t$  is shown in Figure 15 which follows pseudo-first-order reaction kinetics,  $k$  was calculated to be  $0.183 \text{ min}^{-1}$  for CoS@MorphcdtH NPs while for CoS@4-MPipzcdtH NPs the rate constant is  $0.189 \text{ min}^{-1}$  with reduction time of 10 min and 11 min at room temperature respectively. The catalyst used in the reaction was a noble catalyst, it was important to study the recycling of this catalyst. The catalyst loaded for the first catalytic reaction was treated with chloroform and loaded back into the reactor for subsequent tests. The catalyst recycling experiments were performed at 298.15 K–305.15 K, and the results are shown in Figure 15. The catalyst was found to retain its activity even after the fourth recycling without affecting the nitrobenzene conversion. However, the selectivity for PAP decreased to 5–7%. This reduction in selectivity may be due to the handling losses of catalyst transfer in the subsequent recycle runs (Figure 16).

The catalytic efficiency and kinetics were found to be better than many of the reported materials. The dose required for the reduction 4-NP to 4-AP in presently studied CoS@MorphcdtH and CoS@4-MPipzcdtH is lesser than that of already reported spherical-shaped

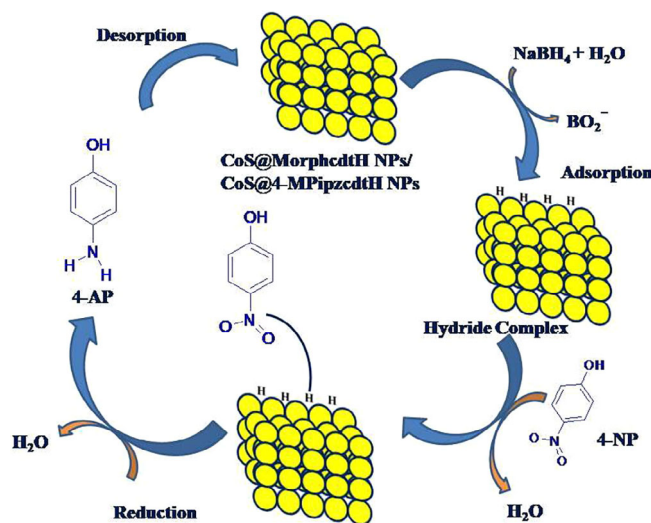


**FIGURE 16** The possible mechanism for the catalytic reduction of 4-NP by  $\text{NaBH}_4$  in presence of the CoS nanocatalyst is suggested as follows: the 4-nitrophenolate anion is bound to the CoS NPs surface by anchoring the two oxygen atoms of the nitro group, after this reaction between the 4-nitrophenolate anion and  $\text{BH}_4^-$  occurs on the surface of CoS nanocatalyst. The two adsorbates are connected by the CoS nanocatalyst's surface in such a way so that electrons can be moved from the oxidation site to the reduction site.

$\text{Fe}_3\text{O}_4@\text{SiO}_2\text{-Ag}$  (NPs dose: 1 g, and degradation rate of  $7.67 \times 10^{-3} \text{ s}^{-1}$ ).<sup>[40]</sup> The presently studied CoS@MorphcdtH and CoS@4-MPipzcdtH has displayed better reusability than that of reported dumbbell-shaped Cu NPs<sup>[41]</sup> and AuNPs@MWCNT NPs.<sup>[42]</sup> Litseacubeba@AuNPs reported

earlier were able to reduce 4-NP to 4-AP at the rate of  $0.348 \text{ min}^{-1}$  and can be reused three times,<sup>[43]</sup> whereas the nanoparticles CoS@MorphcdtH and CoS@4-MPipzcdtH synthesized in the present work displayed better efficiency and can be reused five times with the capability to reduce 4-NP at the rate of  $0.183 \text{ min}^{-1}$  and  $0.189 \text{ min}^{-1}$ , respectively. Jiang et al. reported that the CTAB + PEG-10000@ Ni NPs may be reused for three cycles<sup>[44]</sup> whereas, presently studied nanomaterials CoS@MorphcdtH and CoS@4-MPipzcdtH exhibited better reusability with five cycles. The zero-valent iron nanoparticles (NPs dose: 5–30 mg)<sup>[45]</sup> and nanospheredTA@Fe<sub>3</sub>O<sub>4</sub>-Ag (NPs dose: 3–5 mg)<sup>[46]</sup> were reported to reduce 4-NP for five cycles; the reusability of the iron NPs is comparable to that of the present study (CoS@MorphcdtH and CoS@4-MPipzcdtH).

## 4 | CONCLUSIONS

We have reported chemical reduction method for the fabrication of catalytic efficient CoS@MorphcdtH NPs and CoS@4-MPipzcdtH NPs. With an average size of approximately 12 nm, where carbodithioic acid was used as stabilizer agent respectively. Both CoSNPs acted as a reducing agent due to their unsatisfied oxidation state for the hydrogenation of 4-nitrophenolate. The CoS@MorphcdtH NPs and CoS@4-MPipzcdtH NPs showed excellent application toward the appearance of the peak at 300 nm, possessed excellent stability in aqueous solution, and exhibited superior catalytic activity toward the reduction of NP. The reusability of the catalyst was also performed up to five cycles. This study supports the novel application of CoS@MorphcdtHNPs and CoS@4-MPipzcdtH NPs, for offering an alternative pathway for the reduction of nitro compounds to less toxic amino compounds.

## ACKNOWLEDGMENTS

The authors are grateful to Monika Vats's (Department of Chemistry, Dhanauri (PG) College, Dhanauri, Haridwar-247667 (UK), India) for her assistance during revision which makes manuscript acceptable with high quality as well as Himachal Pradesh University Shimla and Mahari-shi Markandeshwar (Deemed to be University), Mullana, Ambala, for providing facilities and support.

## CONFLICT OF INTEREST STATEMENT

The authors declare that they have no known competing financial interests or personal relationships that could have appeared to influence the work reported in this paper.

## ORCID

Indra Bahadur  <https://orcid.org/0000-0003-2906-473X>

## REFERENCES

- [1] A. K. Gedela, S. G. Naidu, C. Mousumi, *Int. Proc. Chem. Biol. Environ. Eng.* **2015**, *51*, 139.
- [2] T. Aditya, A. Pal, T. Pal, *Chem. Commun.* **2015**, *51*, 410.
- [3] B. Liu, T. Wang, C. Yin, Z. Wei, *J. Mater. Sci.* **2014**, *49*, 5398.
- [4] N. I. Ikhsan, P. Rameshkumar, N. M. Huang, *Electrochim. Acta.* **2016**, *192*, 392.
- [5] R. M. Banik, M. R. Prakash, S. N. Upadhyay, *Sens. Actuat. B: Chem.* **2008**, *131*, 295.
- [6] E. Marais, T. Nyokong, *J. Hazard. Mat.* **2008**, *152*, 293.
- [7] A. O. O'Connor, L. Y. Young, *Environ. Toxicol. Chem.* **1989**, *8*, 853.
- [8] M. S. Dieckmannand, K. A. Gray, *Water Res.* **1996**, *30*, 1169.
- [9] L. L. Bo, Y. B. Zhang, X. Quan, B. Zhao, *J. Hazard. Mat.* **2008**, *153*, 1201.
- [10] N. Modirshahla, M. A. Behnajady, S. Mohammadi-Aghdam, *J. Hazard. Mat.* **2008**, *154*, 778.
- [11] K. C. Hsu, D. H. Chen, *Nanoscale Res. Lett.* **2014**, *9*, 484.
- [12] J. Li, D. Kuang, Y. Feng, F. Zhang, Z. Xu, M. Liu, *J. Hazard. Mater.* **2012**, *201*, 250.
- [13] C. V. Rode, M. J. Vaidya, R. V. Chaudhari, *Org. Process Res. Develop.* **1999**, *3*, 465.
- [14] M. Nasrollahzadeh, Z. Issaabadi, S. M. Sajadi, *RSC Adv.* **2018**, *8*(7), 3723.
- [15] M. Nasrollahzadeh, M. Sajjadi, H. R. Dasmeh, S. M. Sajadi, *J. Alloys and Comp.* **2018**, *763*, 1024.
- [16] M. Nasrollahzadeh, T. Baran, N. Y. Baran, M. Sajjadi, M. R. Tahsili, M. Shokouhimehr, *Sep. and Purif. Technol.* **2020**, *239*, 116542.
- [17] M. Nasrollahzadeh, M. Sajjadi, S. M. Sajadi, *Chin. J. Catal.* **2018**, *39*(1), 109.
- [18] W. H. Arnawtee, B. Jaleh, M. Nasrollahzadeh, R. B. Dehkordi, A. Nasri, Y. Orooji, *Sep. Purif. Technol.* **2022**, *290*, 120793.
- [19] N. C. Z. Moghadam, S. A. Jasim, F. Ameen, D. H. Alotaibi, M. A. L. Nobre, H. Sellami, M. Khatami, *Bioprocess Biosyst. Eng.* **2022**, *45*(7), 1201.
- [20] D. Indhira, M. Krishnamoorthy, F. Ameen, S. A. Bhat, K. Arumugam, S. Ramalingam, S. R. Priyan, G. S. Kumar, *Environ. Res.* **2022**, *212*, 113323.
- [21] F. F. Bobinihi, J. Osuntokun, D. C. Onwudiwe, *J. Saudi. Chem. Soc.* **2018**, *4*, 381.
- [22] G. Gomathi, S. Thirumaran, S. Ciattini, *Polyhedron* **2015**, *102*, 424.
- [23] M. Hrubaru, D. C. Onwudiwe, E. Hosten, *J. Sulfur Chem.* **2016**, *37*, 37.
- [24] S. B. Kalia, D. Kumar, M. Sharma, J. Christopher, *J. Therm. Anal. Calorim.* **2015**, *120*, 1099.
- [25] G. Chauhan, M. Sharma, *Asian J. Chem.* **2022**, *34*, 331.
- [26] E. Vijayakumar, A. Subramania, Z. Fei, P. J. Dyson, *RSC Adv.* **2015**, *5*, 52026.
- [27] A. Pourahmad, S. Sohrabnezhad, *Mat. Lett.* **2011**, *65*, 205.
- [28] P. Scherrer, *Gott. Nachar.* **1918**, *2*, 98.
- [29] S. B. Sibokoza, M. J. Moloto, N. Moloto, P. N. Sibiyi, *Chalco-genide Lett.* **2017**, *14*(2), 69.
- [30] Q. Wang, L. Jiao, H. Du, W. Peng, Y. Han, D. Song, Y. Si, Y. Wang, H. Yuan, *J. Mat. Chem.* **2011**, *21*, 285.

- [31] S. Kundu, M. D. Mukadam, S. M. Yusuf, M. Jayachandran, *Cryst. Eng. Comm.* **2013**, *15*, 482.
- [32] G. Yang, D. Gao, Z. Shi, Z. Zhang, J. Zhang, J. Zhang, D. Xue, *J. Phys. Chem. C* **2010**, *114*, 11477.
- [33] S. Wunder, Y. Lu, M. Albrecht, M. Ballauff, *ACS Catal.* **2011**, *1*, 908.
- [34] J. Safari, A. E. Najafabadi, Z. Zarnegar, S. F. Masoule, *Green Chem. Lett. Rev.* **2016**, *9*, 1.
- [35] W. H. Arnawtee, B. Jaleh, M. Nasrollahzadeh, R. Bakhshali-Dehkordi, A. Nasri, Y. Orooji, *Sep. Purif. Technol.* **2022**, *290*, 120793.
- [36] Y. Lu, Y. Mei, M. Drechsler, M. Ballauff, *Angew. Chem. Int. Ed.* **2006**, *45*, 813.
- [37] S. Panigrahi, S. Basu, S. Praharaj, S. Pande, S. Jana, A. Pal, S. K. Ghosh, T. J. Pal, *J. Phys. Chem. C* **2007**, *111*, 4596.
- [38] B. Baruah, G. J. Gabriel, M. J. Akbashev, M. E. Booher, *Langmuir* **2013**, *29*, 4225.
- [39] C. Castaneda, F. Tzompantzi, R. Gomez, *J. Sol-Gel Sci. Technol.* **2016**, *80*, 426.
- [40] Y. Chi, Q. Yuan, Y. Li, J. Tu, L. Zhao, N. Li, X. Li, *J. Colloid Interface Sci.* **2012**, *383*(1), 96.
- [41] X. Huang, Y. J. Li, H. L. Zhou, X. Zhong, X. F. Duan, Y. Huang, *Chem. A Euro. J.* **2012**, *18*, 9505.
- [42] T. M. Abdel-Fattah, A. Wixtrom, *ECS J. Solid State Sci. Technol.* **2014**, *3*(4), M18.
- [43] D. Van-Dat, T. A. Tai, N. Thanh-Danh, N. Van-Cuong, C. Xuan-Thang, T. N. Lan-Huong, L. V. Thuan, *J. Nanomat.* **2020**, *2020*, 4548790.
- [44] Z. Jiang, J. Xie, D. Jiang, X. Wei, M. Chen, *Cryst. Eng. Comm.* **2013**, *15*, 560.
- [45] K. Sravanthi, D. Ayodhya, P. Y. Swamy, *Mat. Sci. Energy Technol.* **2019**, *2*, 298.
- [46] A. Sangili, M. Annalakshmi, S. M. Chen, P. Balasubramanian, M. Sundrarajan, *Composit. Part B* **2019**, *162*, 33.

**How to cite this article:** G. Chauhan, S. Chauhan, S. Soni, A. Kumar, D. S. Negi, I. Bahadur, *J. Chin. Chem. Soc.* **2023**, *70*(4), 879.  
<https://doi.org/10.1002/jccs.202200459>